Pharm Res (2011) 28:1328–1337
DOI 10.1007/s11095-011-0406-9

RESEARCH PAPER

Non-viral Delivery of Inductive and Suppressive Genes to Adipose-Derived Stem Cells for Osteogenic Differentiation

Anusuya Ramasubramanian • Stacey Shiigi • Gordon K. Lee • Fan Yang

Received: 23 November 2010 / Accepted: 21 February 2011 / Published online: 19 March 2011

ABSTRACT

Purpose To assess the effects of co-delivering osteoinductive DNA and/or small interfering RNA in directing the osteogenic differentiation of human adipose-derived stem cells (hADSCs) using a combinatorial, non-viral gene delivery approach.

Methods hADSCs were transfected using combinations of the following genes: *BMP2*, si*GNAS* and si*Noggin* using poly(β-amino esters) or lipid-like molecules. A total of 15 groups were evaluated by varying DNA doses, timing of treatment, and combinations of signals. All groups were cultured in osteogenic medium for up to 37 days, and outcomes were measured using gene expression, biochemical assays, and histology.

Results Biomaterials-mediated gene delivery led to a dose-dependent up-regulation of *BMP2* and significant gene silencing of *GNAS* and *Noggin* in hADSCs. *BMP2* alone slightly up-regulates osteogenic marker expression in hADSCs. In contrast, co-delivery of *BMP2* and si*GNAS* or si*Noggin* significantly accelerates the hADSC differentiation towards osteogenic differentiation, with marked increase in bone marker expression and mineralization.

Conclusions We report a combinatorial platform for identifying synergistic interactions among multiple genetic signals associated with osteogenic differentiation of hADSCs. Our results suggest that inductive or suppressive genetic switches interact in a complex manner, and highlight the promise of combinatorial approaches towards rapidly identifying optimal signals for promoting desired stem cell differentiation.

KEY WORDS BMP2 · combinatorial · gene delivery · GNAS · Noggin

ABBREVIATIONS

ADSCs	adipose-derived stem cells
ALP	alkaline phosphatase
BMP	bone morphogenetic protein
Cbfa1	core binding factor alpha-1
ELISA	enzyme-linked immunosorbent assay
GNAS	guanine nucleotide binding protein alpha stimulating activity polypeptide
OCN	osteocalcin

Electronic Supplementary Material The online version of this article (doi:10.1007/s11095-011-0406-9) contains supplementary material, which is available to authorized users.

A. Ramasubramanian
Program of Biomechanical Engineering, Stanford University
Stanford, California 94305, USA

S. Shiigi • F. Yang
Department of Bioengineering, Stanford University
Stanford, California 94305, USA

G. K. Lee
Division of Plastic and Reconstructive Surgery
Stanford University Hospital and Clinics
Stanford, California 94305, USA

F. Yang
Department of Orthopaedic Surgery, Stanford University
Stanford, California 94305, USA

F. Yang (✉)
Department of Orthopaedic Surgery and Bioengineering
Stanford University School of Medicine
300 Pasteur Dr., Edwards R105
Stanford, California 94305-5341, USA
e-mail: fanyang@stanford.edu

PBAE poly(β-amino ester)
qRT-PCR quantitative real-time polymerase chain reaction

INTRODUCTION

Bone loss is a significant medical problem and may be caused by traumatic events, fractures, or disease conditions (1). Conventional treatment often involves harvesting autologous bone from the patient for the repair of a defect site or using allograft tissues. Although bone grafting is a well-established surgical technique, there are limitations such as donor site morbidity, insufficient donor tissue supply, dependency on the recipient site for vascularization, and potential immunogenicity. Tissue engineering provides a promising alternative for repairing bony defects by growing biological tissues to restore the lost bone structure and function. Adipose-derived stem cells (ADSCs) represent an attractive cell source for bone regeneration due to their relative abundance, ease of isolation, high proliferation in culture and potential to differentiate towards mesenchymal lineages (2–5). The use of ADSCs for osteogenic differentiation has been reported both *in vitro* and *in vivo* (2,3,6,7) using supplementation of exogenous growth factors such as bone morphogenetic protein-2 (*BMP2*) (8). However, previous work often requires supraphysiological concentration of *BMP2* to obtain osteoblastic differentiation and bone regeneration (4,7). Clinical translation of *BMP2*-mediated bone tissue regeneration is limited by the high cost of growth factor, short half-lives *in vivo*, and potential for unregulated bone formation *in vivo*.

Gene therapy offers a promising approach for promoting lineage-specific differentiation by up-regulating inductive genes via DNA delivery and/or down-regulating inhibitory genes via RNA interference delivery (9,10). Previous reports have shown that *BMP*-transduced ADSCs using adenovirus led to overexpression of *BMP2* and enhanced bone formation *in vivo* (3). A recent study examined the effects of co-delivering two osteogenic lineage activator genes, *BMP2* and core binding factor alpha 1 (*Cbfa1*), also known as *Runx2*, on osteogenic differentiation of ADSCs (4). *BMP2* and *Cbfa1* transduced ADSCs showed a graduated increase in alkaline phosphatase (ALP) activity, up-regulation of osteogenic markers, and increased mineralization. Co-delivery of *BMP2* and dexamethasone also led to increased ALP activity in mouse embryonic stem cells (11). These results suggest that co-delivery of multiple signals may act synergistically to accelerate stem cell differentiation. While extensive work has been performed on delivery of inductive genes for promoting stem cell differentiation, efforts on employing inhibitory gene delivery to enhance stem-cell differentiation are only beginning to emerge (10). RNA interference is a gene-silencing mechanism that involves double-stranded RNA-mediated sequence-specific mRNA degradation and is a powerful mechanism for controlling cell behavior. Zhao *et al.* screened a synthetic siRNA library targeting 5,000 human genes, which yielded 12 candidate suppressors for osteogenic specification, including *GNAS*, in human mesenchymal stem cells (12). Wan *et al.* showed that down-regulation of *BMP* antagonist *Noggin* in osteoblasts enhanced *in vitro* osteogenesis and accelerated *in vivo* bone formation (13). These studies demonstrate the promise of using RNAi-based mechanisms to regulate cell behavior for tissue regeneration.

Despite the potential of gene therapy for tissue engineering, most previous studies relied on viral vectors for efficient gene delivery, which are limited by safety concerns such as potential for mutagenesis, carcinogenesis, immunogenicity and toxicity (14). Furthermore, while stem cells are often exposed to a combination of both inductive and suppressive signals *in vivo*, most previous studies focused on examining stem cell responses to only one type of signal. Therefore, how stem cells respond to interactive genetic signaling remains poorly understood. The aim of this study was to develop a combinatorial platform to facilitate evaluating the effects of co-delivering multiple inductive and suppressive genes on osteogenic differentiation of hADSCs using biomaterial-mediated, non-viral vectors. Specifically, ADSCs were treated with combinations of varying doses of *BMP2* DNA and/or siRNAs of two suppressive genes reported by previous studies, *GNAS* (12,15) and *Noggin* (13). DNA transfection was performed using optimized poly(β-amino esters) (PBAE), a hydrolytically biodegradable polymer that can condense DNA to form nanoparticles (16). siRNA delivery was accomplished using lipid-like molecules as previously reported (17,18). To evaluate the effects of timing and duration of gene delivery on ADSC osteogenic differentiation, three groups received dual treatment of si*Noggin* and *BMP2* DNA delivery at a later time point. All groups were cultured in osteogenic conditions for up to 37 days, and outcomes were analyzed using quantitative gene expression, biochemical assays, cell proliferation and histology.

MATERIALS AND METHODS

Materials

All cell culture reagents and chemicals were purchased from Invitrogen (Carlsbad, CA) and Sigma-Aldrich (St. Louis, MO) unless noted otherwise. The *GNAS*- and *Noggin*-targeting siRNAs were purchased from Applied Biosystems (Foster City, CA).

Cell Culture

Human adipose-derived stem cells (hADSCs) were isolated from excised human adipose tissue of informed and consenting patients following procedures, as previously described (2). hADSCs were cultured in growth medium consisting of Dulbecco's minimal essential medium (DMEM, Invitrogen) supplemented with 10% (*v*/*v*) fetal bovine serum (FBS), 100 units/ml penicillin and 100 µg/mL streptomycin. hADSCs were subcultured upon 90% confluence until passage 3 before use for all experiments. All groups were cultured in osteogenic medium as previously reported (19) for up to 35 days to induce osteogenic differentiation. hADSCs undergoing the same culture condition without any transfection were included as a negative control group (untreated cells) for comparison.

Transfection

Passage 3 hADSCs were seeded at 12,000 cells per well in clear 96-well plates and cultured in growth media at 37°C and 5% CO_2 24 h before transfection. Lipidoid NA114 (Fig. 1a) was synthesized and used for siRNA complexation as previously described (18). Briefly, cells in each well of a 96-well plate were transfected with either 50 ng *GNAS* siRNA, 50 ng *Noggin* siRNA, or a combination of *GNAS*/*Noggin* siRNAs (50 ng of each) complexed with the NA114 lipidoid at lipidoid/siRNA weight ratios of 5:1. Lipidoid/siRNA mixture was incubated for 20 min at room temperature to allow for optimal complexation and then added to cells cultured in growth medium containing 10% FBS. Twenty-four hours after the siRNA treatment, cells were transfected with the *BMP2* DNA using PBAE C32-122 polymer (Fig. 1b) as previously described (16,20). Complexed at room temperature at a weight ratio of 30:1, PBAE/DNA nanoparticles were added to cells at a final DNA dosage of 0.48 µg/well or 0.72 µg/well in a 96-well plate. Cells were incubated with PBAE/DNA nanoparticles for 4 h, and nanoparticle solutions were then removed and replaced with fresh osteogenic medium. To evaluate the timing and duration of gene delivery, three groups received a second round of *Noggin* siRNA delivery at day 11 and *BMP2* delivery at day 12 following the same procedure as described above (Fig. 1c).

RNA Extraction and Real-Time Quantitative Reverse Transcription-Polymerase Chain Reaction

To verify the transfection efficiency in hADSCs using biomaterials-mediated non-viral gene delivery, RNA was extracted from four wells for each group at day 5 using Fastlane® Cell One-Step Buffer Set (Qiagen, Valencia, CA). Quantitative RT-PCR was performed to determine mRNA expression levels of three target genes including

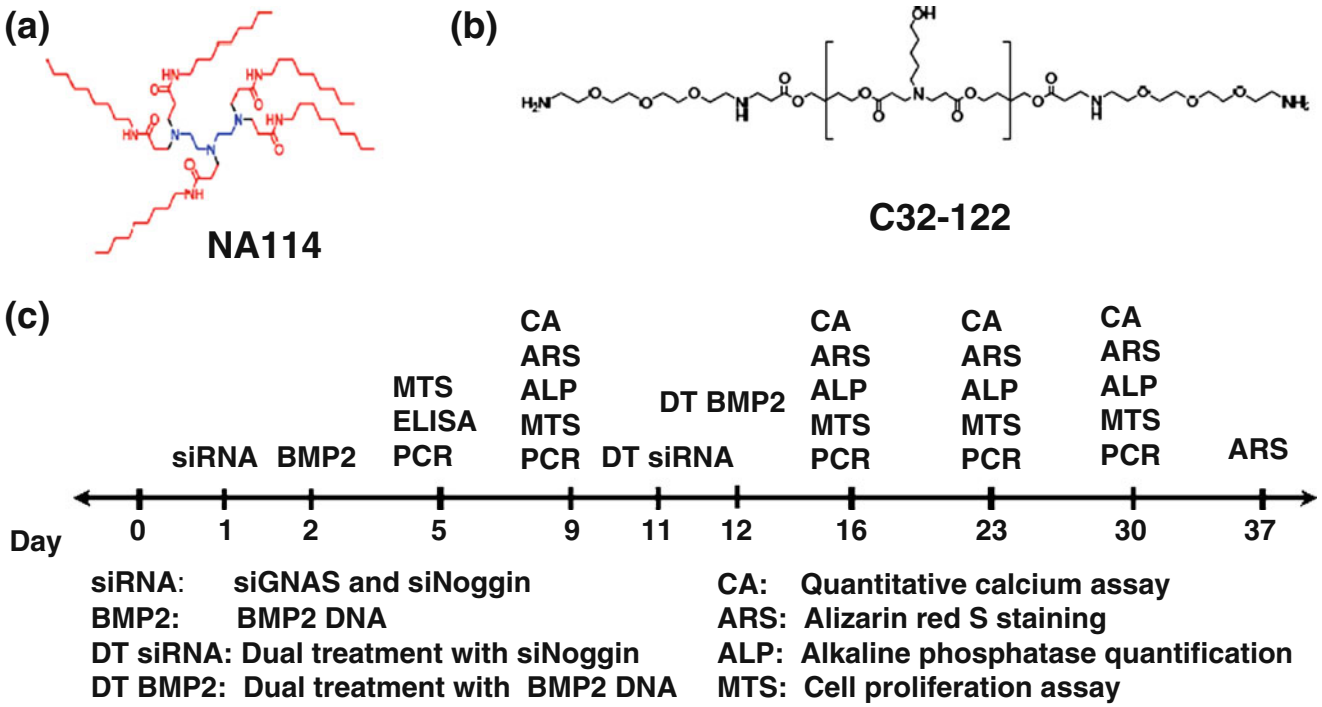

Fig. 1 (**a**) Structure of NA114 lipidoid used for siRNA delivery; (**b**) structure of the C32-122 polymer used for DNA delivery of *BMP2*; (**c**) overview of the experimental design and assays conducted at the various time points.

BMP2, *GNAS*, and *Noggin* using FastLane Cell SYBR Green kit (Qiagen). To evaluate osteogenic differentiation status, RNA extraction was performed in all groups, and real-time PCR was performed at day 9 and day 30 to quantify gene expressions of early bone marker *Cbfa1* and mature bone marker *osteocalcin* (*OCN*). All primers were purchased from MWG Biotech AG (Huntsville, AL), and primer sequences are listed in Table I. All samples were run for 40 PCR cycles on Applied Biosystems 7500 Real-Time PCR System (Carlsbad, CA). Relative expression level of target genes was determined using the comparative C_T method, in which target gene expression was first normalized to an endogenous gene (*GAPDH*), followed by a second normalization to the mRNA level measured in the control group (untreated cells).

Histology

Alizarin red S staining (ARS) and alkaline phosphatase (ALP) staining were performed to evaluate the bone matrix production status. Eight wells from each group were fixed with 10% (*v*/*v*) formaldehyde in PBS for 15 min at room temperature. Cells were successively washed with deionized H_2O and treated with either 40 mM ARS stain (pH 4.1) or ALP reagent prepared using the BCIP/NBT Alkaline Phosphatase Substrate Reagent IV kit (Vector Laboratories, Burlingame, CA). Cells were incubated at room temperature for 30 min with the staining solution prior to washing and imaging. ALP staining was performed on day 23; ARS staining was performed on day 37.

Cell Proliferation

To determine the effects of combinatorial gene delivery on cell proliferation, hADSCs were harvested for cell counting at multiple time points (day 5, 9, 16, 23 and 30) using CellTiter 96® AQ_{ueous} One Solution Cell Proliferation Assay (Promega, Madison, WI) following manufacturer's protocol. The cells were incubated for 4 h at 37°C and 5% CO_2, and absorbance was read every hour for 4 h at 490 nm using a microplate reader. A standard curve was generated using known cell numbers. Experimental cell counts were subsequently calculated by comparing the absorbance to the standard curve.

Table I Primer Sequence Used in RT-PCR

Human Gene	Primer Sequence
GAPDH	F-ACAGTCAGCCGCATCTTCTT
	R-CGACCAAATCCGTTGACTC
GNAS	F-CGTCCCCGGATCCCCTTCC
	R-TCCTCTTCGCCGCCCTCTCC
Noggin	F-CTCGGGGGC
	R-GCACGAGCACTTGCACTCG
BMP2	F-GCAGGTGGGAAAGTTTTGATG
	R-CCTCCAAGTGGGCCACTTC
CBFA1/RUNX2	F-GTGCGGTGCAAACTTTCTCC
	R-AATGACTCGGTTGGTCTCGG
OSTEOCALCIN	F-CCGGGAGCAGTGTGAGCTTA
	R-TAGATGCGTTTGTAGCGGTC

Biochemical Assays

BMP2 Enzyme-Linked Immunosorbent Assay (ELISA)

BMP2 production from hADSCs in the medium supernatant was quantified with a human *BMP2* ELISA Development Kit (PeproTech; Cat 900-K255, Rocky Hill, NJ) following manufacturer's instructions. Cell culture medium was replaced with serum-free DMEM 24 h prior to assay to collect BMP2 secretion for ELISA measurement.

ALP Activity Quantification

To quantify the production of ALP, cells were first lysed using 0.2% Triton X-100 in PBS. Enzyme activity in the lysate was determined using the ALP reagent containing p-nitrophenylphosphate (Pointe Scientific, Canton, MI) following manufacturer's instructions. Absorbance was measured at 405 nm using a microplate reader. ALP activity for each sample was normalized to the respective average cell counts, determined using the cell proliferation assay. ALP activity was determined on day 9, 16, 23 and 30.

Calcium Quantification

Cells were washed 3 times with Mg^{2+}- and Ca^{2+}-free PBS followed by incubation with 0.6 N HCl for 24 h at 4°C. The calcium content in the supernatant was determined with the Calcium Reagent Kit (Pointe Scientific, Canton, MI) based on the reaction of calcium with o-cresolphthalein complexone and standard curve. The colorimetric reaction was read at 570 nm on a microplate reader.

Statistical Analysis

Statistical significance was determined using Dunnet's Multiple Comparison Test, a repeated measure of ANOVA. All experiments were performed in triplicate, and all data are presented as mean ± SD, with $p<0.05$ considered to be statistically significant. The statistical software package Prism 5.0c (GraphPad Software, San Diego, CA) was used to aid data analysis.

RESULTS

BMP2 Transfection Efficiency

To determine the *BMP2* transfection efficiency, mRNA transcript levels were determined using quantitative RT-PCR at day 5 (Fig. 2). Groups treated with *BMP2* alone exhibited a dose-dependent increase in *BMP2* mRNA transcript level, with over 55-fold increase in the high dosage group (0.72B group) compared to the control. Groups that received co-delivery of *BMP2* and siRNAs (si*GNAS*, si*Noggin* or both) also showed a dose-dependent up-regulation of *BMP2* signals, although the increase is much lower compared to the groups transfected with *BMP2* alone. Co-delivery of all three genetic signals significantly decreased the *BMP2* up-regulation to a level comparable to the control group. All groups treated with *BMP2* DNA produced detectable level of *BMP2*, while the control (untransfected cells) or cells treated with si*GNAS* did not produce detectable levels of *BMP2* (Fig. 3). Inhibiting *Noggin* also led to a detectable level of *BMP2*, while such effect was abolished when cells were co-delivered with siRNA for *GNAS* and *Noggin* (G/N group). *BMP2* protein level reached a peak at the intermediate *BMP2* dosage group (0.48B group) and decreased at the high *BMP2* dosage group (0.72B group).

siRNA Transfection Efficiency

Quantitative gene expression analysis was performed for *Noggin* and *GNAS* at day 5 to determine the siRNA knockdown efficiency (Fig. 4). Groups treated with si*Noggin* alone exhibited significant gene silencing efficiency (~70%).

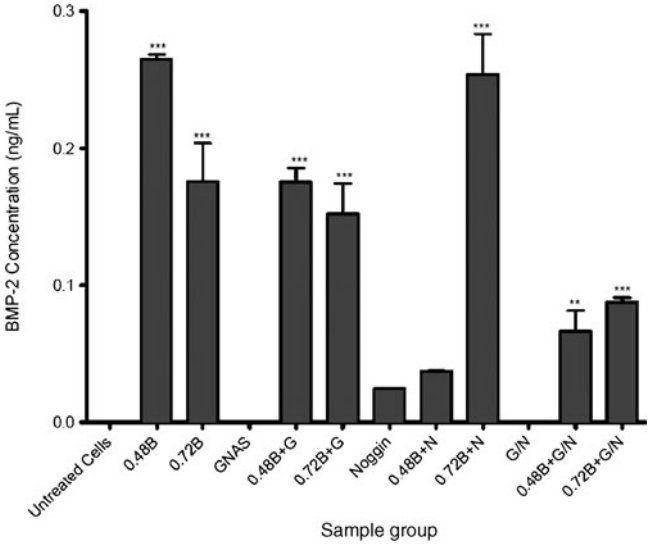

Fig. 3 *BMP2* production at protein level by ADSCs (mean transcripts ± SD, $n=3$) at Day 5. Significance is expressed as follows: ***, $p<0.001$; **, $p<0.01$; *, $p<0.05$ compared to the untreated, control hADSCs. B: *BMP2*; G: *GNAS*; N: *Noggin*; G/N: Co-delivery of *GNAS* and *Noggin*.

Co-delivery of si*Noggin* and *BMP2* abolished the gene silencing effects observed with si*Noggin* alone. In fact, it led to an increased *GNAS* and *Noggin* mRNA transcript level. Cells treated with si*GNAS* exhibited the highest *Noggin* transcript levels. All groups treated with si*GNAS* exhibited significant *GNAS* knockdown including groups that received co-delivery of other signals. Knockdown efficiencies ranged from approximately 85% for groups co-delivered with si*GNAS* and si*Noggin* (G/N group) to approximately 60% for hADSCs treated with si*GNAS* alone or with *BMP2* and si*GNAS*. In contrast, samples treated with co-delivery of

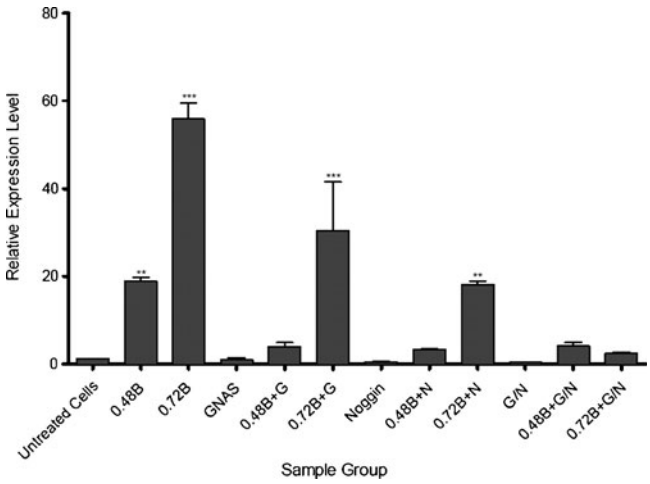

Fig. 2 Quantitative gene expression of hBMP2 by ADSCs (mean ± SD, $n=3$) at Day 5. Significance is expressed as follows: ***, $p<0.001$; **, $p<0.01$; *, $p<0.05$ compared to the control (untreated cells). B: *BMP2*; G: *GNAS*; N: *Noggin*; G/N: Co-delivery of *GNAS* and *Noggin*. DNA dose: μg per well in a 96-well plate.

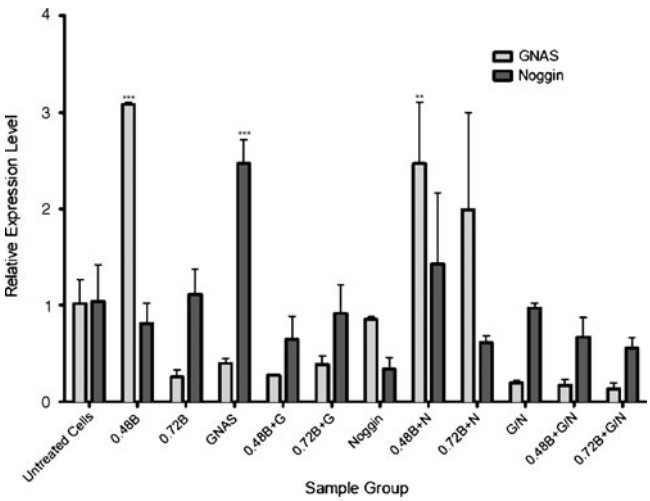

Fig. 4 Remaining mRNA expression level of inhibitory target genes (*GNAS* and *Noggin*) (mean ± SD, $n=3$) at day 5. ***: $p<0.001$; **: $p<0.01$; *: $p<0.05$ compared to the untreated, control hADSCs. B: *BMP2*; G: *GNAS*; N: *Noggin*; G/N: Co-delivery of *GNAS* and *Noggin*.

BMP2 and si*Noggin* exhibited 1–2-fold increased *GNAS* transcript levels compared to the untreated, control group.

Effects of Combinatorial Gene Delivery on Osteogenic Marker Expressions

To determine the effect of combinatorial non-viral gene delivery on osteogenic differentiation, qRT-PCR was performed for the early bone marker *Cbfa1* and mature bone marker *OCN* (Figs. 5 and 6). Several groups demonstrated a peak *Cbfa1* expression at day 9, followed by a decrease in expression levels by day 30. In general, combinatorial gene delivery resulted in an increase of *Cbfa1* expression compared to the control group. For example, groups treated with *BMP2* and si*GNAS* (0.48B + G group) or si*Noggin* (0.48B + N group) showed over 10-fold increase in *Cbfa1* expression than groups treated with either *BMP2* alone or si*GNAS* alone. We also noted that peak expression was reached at different time points in different groups. For example, co-delivery of *BMP2* with si*GNAS* (0.48B + G group) led to early peak of *Cbfa1* expression, while co-delivery with si*Noggin* (0.48B + N group) led to peak expression of *Cbfa1* at day 30. Interestingly, cells treated with si*GNAS* or si*Noggin* alone showed opposite patterns. Specifically, cells treated with si*Noggin* reached *Cbfa1* peak expression at day 9, but dropped by day 30. In contrast, si*GNAS*-treated cells showed low *Cbfa1* expression at day 9, followed by a 4-fold higher *Cbfa1* expression at day 30.

The expression of *OCN*, the mature bone marker, demonstrated a similar trend as *Cbfa1* expression. Co-delivering lower dose of *BMP2* and si*Noggin* (0.48B + N group) results in over 10-folds higher expression of both *OCN* and *Cbfa1* compared to the control group. Similarly, co-delivery of *BMP2* and si*GNAS* led to an early upregulation of *OCN* at day 9 while co-delivery of *BMP2* and si*Noggin* led to a later up-regulation of *OCN* at day 30. Samples treated with si*GNAS* alone expressed a five-fold increase in *OCN* expression at day 30, while treatment with si*Noggin* resulted in the opposite effect. Cells treated with co-delivery of si*GNAS* and si*Noggin* exhibited only a marginal increase in *OCN* compared to the control group at day 30.

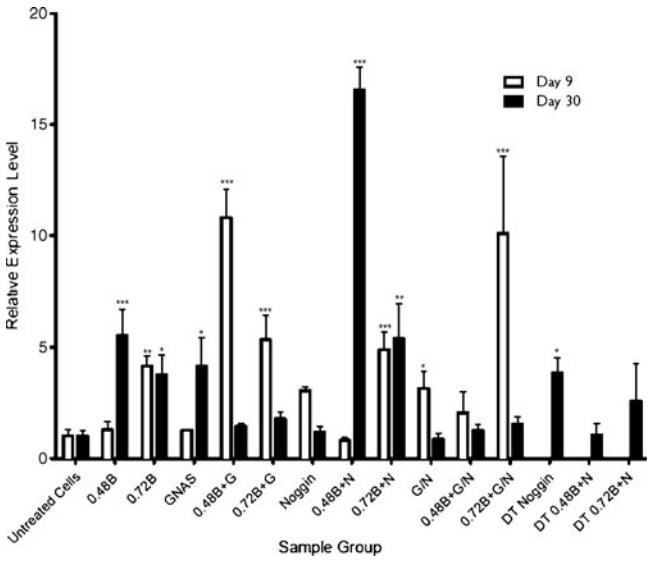

Fig. 5 Quantitative gene expression for early bone marker, Cbfa1, (mean transcripts ± SD, $n=3$) at Day 9 & 30. ***: $p<0.001$; **: $p<0.01$; *: $p<0.05$ compared to the control (untreated cells). B: *BMP2*; G: *GNAS*; N: *Noggin*; G/N: Co-delivery of *GNAS* and *Noggin*.

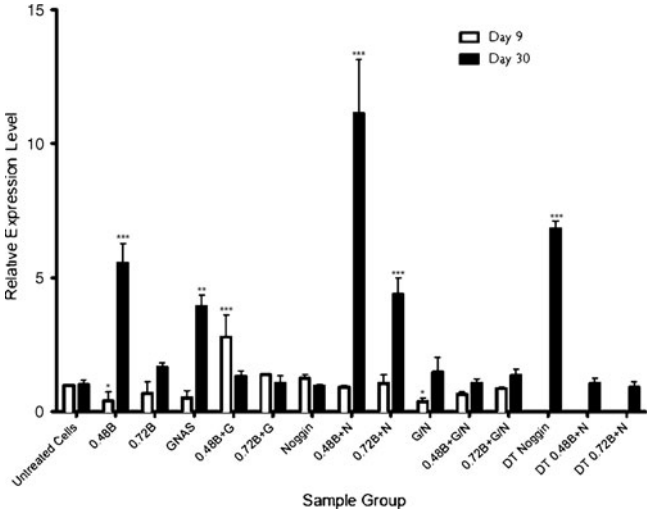

Fig. 6 Quantitative gene expression for late bone marker osteocalcin, (mean ± SD, $n=3$) at Day 9 & 30. ***: $p<0.001$; **: $p<0.01$; *: $p<0.05$ compared to the untreated hADSCs. B: *BMP2*; G: *GNAS*; N: *Noggin*; G/N: Co-delivery of *GNAS* and *Noggin*.

Histology

Staining for mineralization was performed using ARS staining at day 37 (Fig. 7). ADSCs transfected with *BMP2* alone showed only modest mineralization, while siRNA treatment led to strong staining overall. However, *BMP2* seems to have a potent stimulating effect when co-administered with siRNAs. For example, cells treated with 0.48μg/well of *BMP2* and si*GNAS* (0.48B + G group) and 0.48μg/well of *BMP2*, si*GNAS* and si*Noggin* (0.48B + G/N group) showed intense mineralization at day 37. Furthermore, groups that exhibited early upregulation of *OCN* transcript (by day 9), such as groups treated with si*Noggin* (Noggin group) or 0.48μg/well of *BMP2* and si*GNAS* (0.48B + G group), also showed more pronounced ARS staining. While most groups showing upregulation of *OCN* transcript by day 9 demonstrated more pronounced ARS staining, cells treated with a higher dose of *BMP2* exhibited poor staining despite high levels of *OCN* and its precursor, *Cbfa1*. These groups had fewer cells than single-treatment groups due to additional

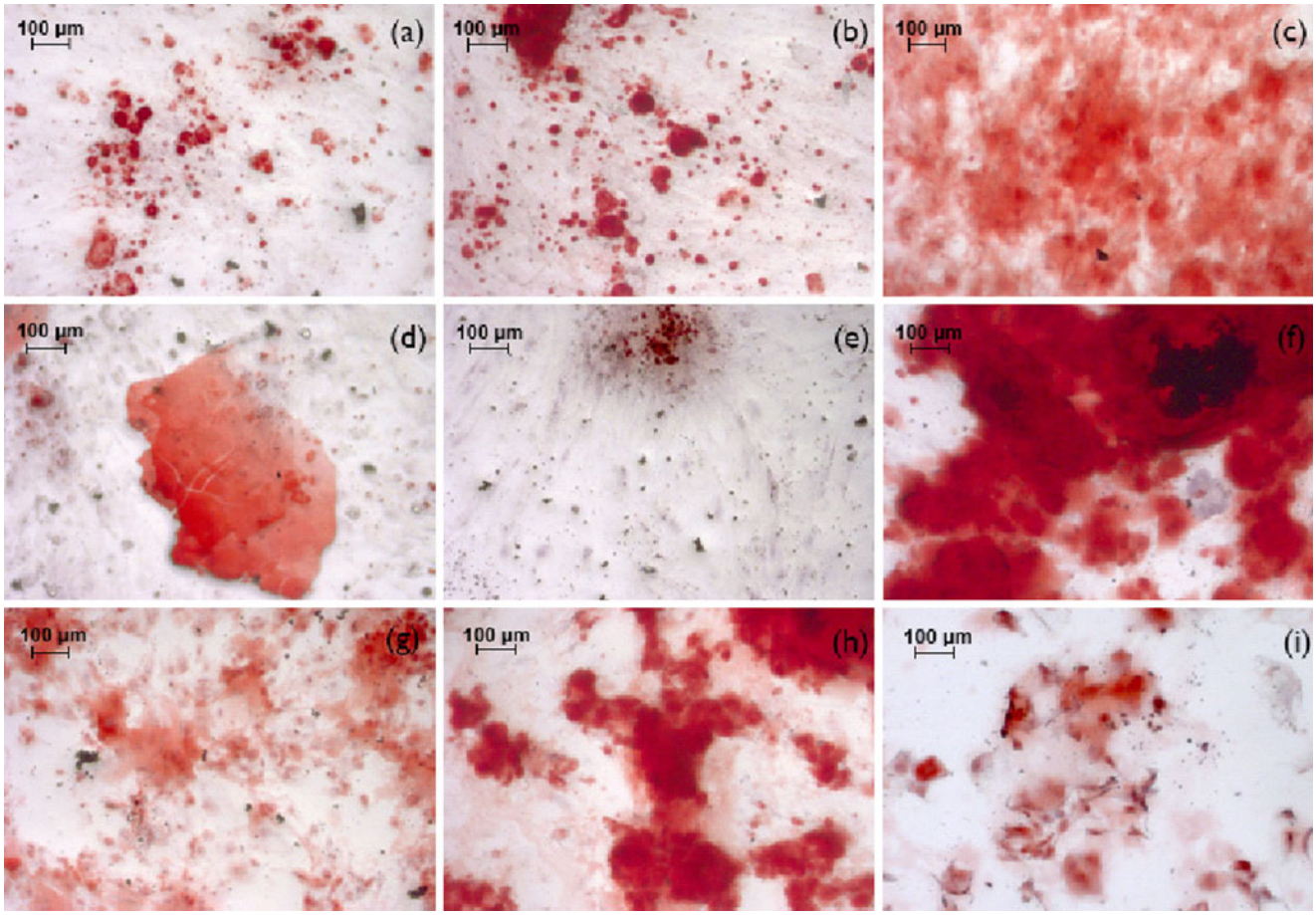

Fig. 7 Alizarin red S staining at day 37 for evaluation of mineralization. (**a**) untransfected ADSCs, (**b**) *GNAS*, (**c**) *Noggin*, (**d**) 0.48B, (**e**) 0.72B, (**f**) 0.48B + G, (**g**) 0.48B + N, (**h**) 0.48B + G/N, (**i**) 0.72B + G/N. B: *BMP2*; G: *GNAS*; N: *Noggin*; G/N: Co-delivery of *GNAS* and *Noggin*. DNA dose: µg per well in a 96-well plate.

toxicity (Fig. 8). The lower dose of *BMP2* co-delivered with si*GNAS* or si*Noggin* is sufficient to induce osteogenic differentiation more efficiently than the control.

Cell Proliferation

Cell proliferation was measured over 30 days for all treatment groups. At day 5, groups transfected with the higher dosage of *BMP2* (0.72B group) exhibited significantly higher toxicity compared to the lower dosage *BMP2* group (0.48B group) (Fig. 8). Cell proliferation increased steadily over time, and by day 23, no significant difference in cell number was observed. Cell proliferation was the highest between day 9 and day 16, with ~4-fold increase in cell number in all groups.

DISCUSSION

Osteogenic differentiation of stem cells is tightly regulated by a complex network of signaling pathways. Most of the work so far has focused on delivery of osteoinductive

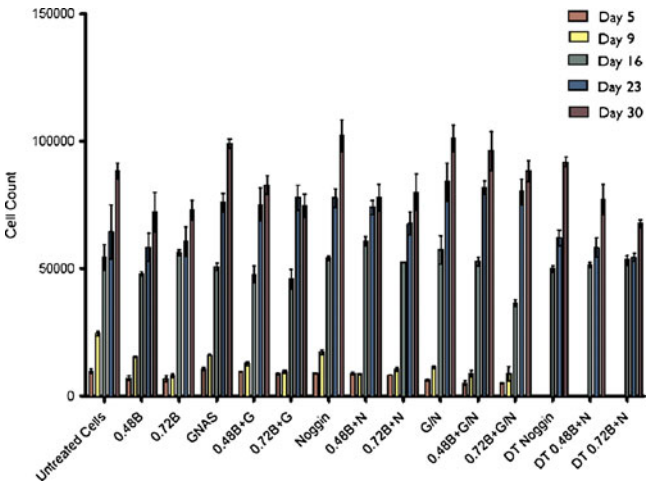

Fig. 8 Cell proliferation of transfected hADSCs (mean ± SD, $n = 4$) over 30 days. B: *BMP2*; G: *GNAS*; N: *Noggin*; G/N: Co-delivery of *GNAS* and *Noggin*; DT: Dual treatment.

signals, such as recombinant *BMP2* growth factor or *BMP2* DNA, to induce bone differentiation (3). More recently, gene silencing of osteogenic suppressors has also been explored to enhance osteogenic differentiation in osteoblasts and bone marrow-derived stem cells (12,13,21). While these studies have identified potential individual gene targets involved in directing osteogenic differentiation, how these signals interact with each other to modulate stem-cell differentiation remains largely unknown. A combinatorial screening platform may provide a valuable tool to help elucidate both the complex interactions within a signaling network and the mechanisms underlying lineage-specific differentiation. As a proof-of-principle study, here we focused on examining the effects of three osteogenic regulators, *BMP2*, si*GNAS*, and si*Noggin*, on directing hADSCs towards osteogenic differentiation. Such a miniaturized, combinatorial screening platform allows examination of a relatively large number of treatments with significantly reduced materials, cells, and cost.

Current gene delivery methods rely on one of two types of vectors: viral or non-viral vectors (polymeric or lipid-based carriers). Biomaterials-based vectors are potentially safer but often suffer from low transfection efficiency (22). In particular, it has been a challenge to transfect human primary stem cells using current commercially available transfection reagents such as FuGene (3%) and DOTAP (5%) (23). To overcome this hurdle, combinatorial polymer synthesis and high-throughput screening have been employed to facilitate the development of novel non-viral gene delivery systems (12,17,24). Biodegradable nanoparticulate PBAEs and synthetic lipid-like molecules ("lipidoids") are attractive options for non-viral gene delivery of DNA or siRNA to stem cells due to their high transfection efficiency and low toxicity (16,18). Our results demonstrate a dose-dependent up-regulation of the osteoinductive gene, *BMP2*, at the mRNA level. The *BMP2* secretion at the protein level also showed a significant increase, with the highest *BMP2* production obtained using an intermediate dose of *BMP2* (0.48 μg/well in a 96-well plate). This is likely due to the increased toxicity associated with the higher *BMP2* dosage (Fig. 8). Lipidoid-mediated delivery of *Noggin* and *GNAS*-targeting siRNAs also led to significant silencing of these inhibitory genes.

For many pharmaceutical delivery applications, decreasing the doses and duration of payload delivery may provide benefits such as reduced materials cost and less risk for undesired side effects. Our non-viral-based DNA delivery system offers a much shorter-term gene up-regulation (~7 days) as opposed to viral-mediated *BMP2*, which can last stably for up to 8 weeks *ex vivo* in rat bone marrow-derived mesenchymal stem cells (BMSCs) (25). Furthermore, the *BMP2* production at the protein level using our non-viral system (~0.25 ng/ml) is at least an order of magnitude lower than the protein level induced by viral-mediated *BMP2* delivery (2–8 ng/ml in viral vectors) (4). The fact that we still observed a 5-fold increase in the expressions of bone markers such as *Cbfa1* and *OCN* suggests the potential of achieving therapeutic efficacy with lower doses and shorter time of *BMP2* exposure. Interestingly, ADSCs treated with *BMP2* alone did not show strong mineralization, while co-delivery of *BMP2* with si*GNAS* or si*Noggin* led to a much more intense mineralization (Fig. 7). Recent studies by others report *BMP2*-treated ADSCs did not improve repair of segmental femoral defects (33,34). In our study, we observed a decrease in calcium (Fig. S1) and ALP activity (Fig. S2) in groups treated with *BMP2* DNA at later time points (day 16, 23 and 30) compared to corresponding groups treated with siRNA alone (i.e. *GNAS*, *Noggin* or G/N groups). Together, this suggests that *BMP2* alone at a low dose may not be a potent inductive regulator for osteogenic differentiation of ADSCs (26,27).

Our results also confirm that various inductive or inhibitory genetic switches are tightly interwoven and interact in a complex manner. Human ADSCs treated with si*Noggin* alone led to increased *BMP2* secretion at the protein level. This is consistent with previous reports where suppressing *Noggin* resulted in increased *BMP2* levels in osteoblasts (13). In addition, co-delivery of si*Noggin* and *BMP2* DNA reduced *Noggin* knockdown compared to si*Noggin* alone. This suggests that overexpression of *BMP2* may stimulate the expression of *Noggin* to compensate via a negative feedback-type mechanism (28). Previous work has shown that silencing *GNAS* expression resulted in increased activity of *Cbfa1*, a key transcription factor that controls osteogenic differentiation (21). *Cbfa1* is directly regulated by *GNAS*, while *Noggin* may regulate *Cbfa1* indirectly through *BMP2* and *Smad* protein family expression (12,13,15,29–31,39). Expression of *Cbfa1* was determined on both days 9 and 30 (Fig. 5), and mineralization staining at day 37 largely (Fig. 8) follows the trend observed in day 9 *Cbfa1* expression, confirming that *Cbfa1* is a potent early marker for predicting later osteogenesis. A previous study has reported that *Cbfa1* expression may drop during the later stages of differentiation (13). Similarly, our results show a decrease of *Cbfa1* expression at day 30 in lead groups (0.48B + G, 0.72B + G, *Noggin*, G/N, 0.72B + G/N groups) compared to day 9. We also observed a significant synergy in co-delivery of *BMP2* and si*GNAS* in accelerating the osteogenic differentiation of hADSCs (Figs. 4 and 5), as well as enhancing mineralization (Fig. 6). This may be due to the synergistic upregulation of the transcriptional factor, *Cbfa1*, which is a key regulator of osteoblast differentiation and regulates the downstream expression of mature bone markers (32–38). These results highlight the need for such combinatorial studies to help elucidate the complex interactions among these factors and to facilitate rapid

identification of lead conditions for promoting lineage-specific differentiation.

Co-delivery of multiple genetic signals also seemed to influence the pace of osteogenic differentiation. *BMP2* and si*GNAS* co-delivery or si*Noggin* alone led to accelerated osteogenic differentiation, as shown by an early peak expression of *Cbfa1* at day 9. In contrast, *BMP2* and si*Noggin* co-delivery slowed down the differentiation process, and *Cbfa1* expression did not peak until day 30. This suggests that while both *GNAS* and *Noggin* negatively regulate *Cbfa1*, their relative impact on transcript expression differs (12,13,38). *Cbfa1* is directly regulated by *GNAS*, while *Noggin* may regulate *Cbfa1* indirectly through *BMP2* and *Smad* protein family expression (12,13,15,39).

To evaluate the effects of timing and duration of genetic treatment on hADSCs osteogenesis, we have performed three dual treatment groups (DT *Noggin*, DT 0.48B + N, DT 0.72B + N) on day 11 for si*Noggin* and day 12 for *BMP2* DNA (Fig. 1c). These dual treatment groups offered a longer duration of *BMP* production or *Noggin* inhibition. We did not observe any further increase in bone marker expression in these dual treatment groups compared to the respective control groups receiving a single treatment. In fact, the group with dual treatment of *BMP2* and si*Noggin* showed significant decrease in osteogenic marker expression at day 30 in comparison to the single treatment control (DT 0.48B + N *vs.* 0.48B + N). These results provide valuable information on optimizing the timeline of delivery required for enhanced osteogenic differentiation in hADSCs.

CONCLUSIONS

In summary, we report a combinatorial non-viral gene delivery platform, which targets both inductive and suppressive genes for promoting osteogenic differentiation in hADSCs. Specifically, we explored the interactive signaling of multiple signals involved in the bone differentiation pathway, namely *BMP2*, an inducer of osteogenesis, as well as *GNAS* and *Noggin*, two suppressive genes for osteogenesis. Our results suggest that various inductive or suppressive genetic switches interact in a complex manner. These results also highlight the promise of combinatorial approaches towards rapidly identifying potent combinations of treatments, which may be difficult to predict using conventional, reductionist approaches. Co-delivery of multiple genetic signals under optimized combinations and doses may act synergistically to influence the pace and level of osteogenic differentiation of ADSCs. Importantly, such therapeutic efficacy may be achieved using significantly lower doses and shorter time of delivery. While our study chose to focus on hADSCs and osteogenic differentiation, such combinatorial approach may be adapted for examining the interactive signaling for regulating a broad range of cell types and various cell fate processes.

ACKNOWLEDGEMENTS

This work was supported by a start-up package from Stanford School of Medicine, Stanford Bio-X Interdisciplinary Initiatives Program Grant, and Baxter Faculty Scholar Award to F.Y. from Baxter Foundation. A. R. would like to thank the Stanford Undergraduate Advising and Research Office for funding, and S.S. would like to thank the Gabilan Stanford Graduate Fellowship for financial support.

REFERENCES

1. Mankin HJ. Nontraumatic necrosis of bone (Osteonecrosis). New Engl J Med. 1992;326(22):1473–9.
2. Zuk PA, Zhu M, Mizuno H, Huang J, Futrell JW, Katz AJ, *et al.* Multilineage cells from human adipose tissue: implications for cell-based therapies. Tissue Eng. 2001;7(2):211–28.
3. Dragoo JL, Choi JY, Lieberman JR, Huang J, Zuk PA, Zhang J, *et al.* Bone induction by BMP-2 transduced stem cells derived from human fat. J Orthop Res. 2003;21(4):622–9.
4. Lee SJ, Kang SW, Do HJ, Han I, Shin DA, Kim JH, *et al.* Enhancement of bone regeneration by gene delivery of BMP2/Runx2 bicistronic vector into adipose-derived stromal cells. Biomaterials. 2010;31(21):5652–9.
5. Schaffler A, Buchler C. Concise review: adipose tissue-derived stromal cells—basic and clinical implications for novel cell-based therapies. Stem Cells. 2007;25(4):818–27.
6. Cowan CM, Shi YY, Aalami OO, Chou YF, Mari C, Thomas R, *et al.* Adipose-derived adult stromal cells heal critical-size mouse calvarial defects. Nat Biotechnol. 2004;22(5):560–7.
7. Jeon J, Rhie JW, Kwon IK, Kim JH, Kim BS, Lee SH. *In vivo* bone formation following transplantation of human adipose-derived stromal cells that are not differentiated osteogenically. Tissue Eng A. 2008;14(8):1285–94.
8. Urist MR. Bone: formation by autoinduction. Science. 1965;150(698):893–9.
9. Evans CH, Gouze JN, Gouze E, Robbins PD, Ghivizzani SC. Osteoarthritis gene therapy. Gene Ther. 2004;11(4):379–89.
10. Cheema SK, Chen E, Shea LD, Mathur AB. Regulation and guidance of cell behavior for tissue regeneration via the siRNA mechanism. Wound Repair Regen. 2007;15(3):286–95.
11. Mikami Y, Asano M, Honda MJ, Takagi M. Bone morphogenetic protein 2 and dexamethasone synergistically increase alkaline phosphatase levels through JAK/STAT signaling in C3H10T1/2 cells. J Cell Physiol. 2010;223(1):123–33.
12. Zhao Y, Ding S. A high-throughput siRNA library screen identifies osteogenic suppressors in human mesenchymal stem cells. Proc Natl Acad Sci. 2007;104(23):9673–8.
13. Wan DC, Pomerantz JH, Brunet LJ, Kim JB, Chou YF, Wu BM, *et al.* Noggin suppression enhances *in vitro* osteogenesis and accelerates *in vivo* bone formation. J Biol Chem. 2007;282(36):26450–9.
14. Thomas CE, Ehrhardt A, Kay MA. Progress and problems with the use of viral vectors for gene therapy. Nat Rev Genet. 2003;4(5):346–58.
15. Shore EM, Ahn J, de Beur SJ, Li M, Xu M, Gardner RJM, *et al.* Paternally inherited inactivating mutations of the GNAS1 gene in progressive osseous heteroplasia. N Engl J Med. 2002;346(2):99–106.

16. Yang F, Green JJ, Dinio T, Keung L, Cho SW, Park H, *et al.* Gene delivery to human adult and embryonic cell-derived stem cells using biodegradable nanoparticulate polymeric vectors. Gene Ther. 2009;16(4):533–46.
17. Akinc A, Zumbuehl A, Goldberg M, Leshchiner ES, Busini V, Hossain N, *et al.* A combinatorial library of lipid-like materials for delivery of RNAi therapeutics. Nat Biotechnol. 2008;26 (5):561–9.
18. Cho SW, Goldberg M, Son SM, Xu Q, Yang F, Mei Y, *et al.* Lipid-like nanoparticles for small interfering RNA delivery to endothelial cells. Adv Funct Mater. 2009;19(19):3112–8.
19. Yang F, Williams CG, Wang DA, Lee H, Manson P, Elisseeff J. The effect of incorporating RGD adhesive peptide in polyethylene glycol diacrylate hydrogel on osteogenesis of bone marrow stromal cells. Biomaterials. 2005;26(30):5991–8.
20. Yang F, Cho SW, Son SM, Bogatyrev SR, Singh D, Green JJ, *et al.* Genetic engineering of human stem cells for enhanced angiogenesis using biodegradable polymeric nanoparticles. Proc Natl Acad Sci. 2010;107(8):3317–22.
21. Lietman SA, Ding C, Cooke DW, Levine MA. Reduction in Gs [alpha] induces osteogenic differentiation in human mesenchymal stem cells. Clin Orthop Relat Res. 2005;(434):231–8.
22. Pack DW, Hoffman AS, Pun S, Stayton PS. Design and development of polymers for gene delivery. Nat Rev Drug Discov. 2005;4(7):581–93.
23. Aluigi M, Fogli M, Curti A, Isidori A, Gruppioni E, Chiodoni C, *et al.* Nucleofection is an efficient nonviral transfection technique for human bone marrow-derived mesenchymal stem cells. Stem Cells. 2006;24(2):454–61.
24. Green JJ, Langer R, Anderson DG. A combinatorial polymer library approach yields insight into nonviral gene delivery. Acc Chem Res. 2008;41(6):749–59.
25. Sugiyama O, An DS, Kung S, Feeley BT, Gamradt S, Liu NQ, *et al.* Lenti-virus-mediated gene transfer induces long-term transgene expression of BMP-2 *in vitro* and new bone formation *in vivo*. Mol Ther. 2005;11(3):390–8.
26. Zuk P, Chou YF, Mussano F, Benhaim P, Wu BM. Adipose-derived stem cells and BMP2: Part 2. BMP2 may not influence the osteogenic fate of human adipose-derived stem cells. Connect Tissue Res. 2010 Aug 11 (Epub ahead of print).
27. Chou YF, Zuk P, Chang TL, Benhaim P, Wu BM. Adipose-derived stem cells and BMP2: Part 1. BMP2-treated adipose-derived stem cells do not improve repair of segmental femoral defects. Connect Tissue Res. 2010 Aug 11. (Epub ahead of print).
28. Zhu W, Kim J, Cheng C, Rawlins BA, Boachie-Adjei O, Crystal RG, *et al.* Noggin regulation of bone morphogenetic protein (BMP) 2/7 heterodimer acitivty *in vitro*. Bone. 2006;39(1):61–71.
29. Yang S, Wei D, Wang D, Phimphilai M, Krebsbach PH, Franceschi RT. *In vitro* and *in vivo* synergistic interactions between Runx2/Cbfa1 transcription factor and bone morphogenetic protein-2 in stimulating osteoblast differentiation. J Bone Miner Res. 2003;18(4):705–15.
30. Bertaux K, Broux O, Chauveau C, Hardouin P, Jeanfils J, Devedjian JC. Runx2 regulates the expression of GNAS on SaOs-2 cells. Bone. 2006;38(6):943–50.
31. Lee KS, Kim HJ, Li QL, Chi XZ, Ueta C, Komori T, *et al.* Runx2 is a common target of transforming growth factor beta 1 and bone morphogenetic protein 2, and cooperation between Runx2 and Smad5 induces osteoblast-specific gene expression in the pluripotent mesenchymal precursor cell line C2C12. Mol Cell Biol. 2000;20(23):8783–92.
32. Banerjee C, Hiebert SW, Stein JL, Lian JB, Stein GS. An AML-1 consensus sequence binds an osteoblast-specific complex and transcriptionally activates the osteocalcin gene. Proc Natl Acad Sci USA. 1996;93(10):4968–73.
33. Banerjee C, McCabe LR, Choi JY, Hiebert SW, Stein JL, Stein GS, *et al.* Runt homology domain proteins in osteoblast differentiation: AML3/CBFA1 is a major component of a bone-specific complex. J Cell Biochem. 1997;66(1):1–8.
34. Ducy P, Karsenty G. Two distinct osteoblast-specific cis-acting elements control expression of a mouse osteocalcin gene. Mol Cell Biol. 1995;15(4):1858–69.
35. Ducy P, Zhang R, Geoffroy V, Ridall AL, Karsenty G. Osf2/Cbfa1: a transcriptional activator of osteoblast differentiation. Cell. 1997;89 (5):747–54.
36. Isogai Y, Akatsu T, Ishizuya T, Yamaguchi A, Hori M, Takahashi N, *et al.* Parathyroid hormone regulates osteoblast differentiation positively or negatively depending on the differentiation stages. J Bone Miner Res. 1996;11(10):1384–93.
37. Noda M, Yoon K, Prince CW, Butler WT, Rodan GA. Transcriptional regulation of osteopontin production in rat osteosarcoma cells by type beta transforming growth factor. J Biol Chem. 1988;263(27):13916–21.
38. Kream BE, Rowe DW, Gworek SC, Raisz LG. Parathyroid hormone alters collagen synthesis and procollagen mRNA levels in fetal rat calvaria. Proc Natl Acad Sci USA. 1980;77(10):5654–8.
39. Javed A, Bae JS, Afzal F, Gutierrez S, Pratap J, Zaidi SK, *et al.* Structural coupling of Smad and Runx2 for execution of the BMP2 osteogenic signal. J Biol Chem. 2008;283(13):8412–22.